SOME OBSERVATIONS OF CRACK PROPAGATION AND ARREST IN A SYSTEM WITH AN INCREASING STRESS INTENSITY FACTOR

R.S. Gates*

*Materials Division,
Central Electricity Research Laboratories
Kelvin Avenue, Leatherhead, Surrey KT22 7SE U.K.

ABSTRACT

Crack arrest tests have been performed on double cantilever beam specimens with sharp starting cracks and a loading system that initially produced an increasing driving force for the growing crack. The test thus simulated the loading effects of thermal stresses in a pressure vessel wall. Crack growth and specimen load were monitored during crack growth and a computer analysis used to calculate the dynamic stress intensity factor.

The results were significantly different to those produced from blunt notched specimens. The arrest toughness was similar to or greater than the value of the static fracture toughness determined in the same specimen and crack speeds were low. Blunt notched specimens produced lower values of the arrest toughness and higher crack speeds.

KEYWORDS

Crack propagation; crack arrest; dynamic stress intensity; fracture properties, finite difference; steel.

INTRODUCTION

Common features of most laboratory crack arrest tests (Hoagland, Rosenfield and Hahn 1972; Kobayashi, Emery and Mall 1976; Kalthoff, Beinert and Winkler 1977) are that cracks are initiated from blunt starting notches and that the loading system is effectively displacement controlled. The first condition ensures that the load necessary to initiate fast fracture is elevated above that for a sharp crack and the strain energy stored in the specimen guarantees significant crack growth. The second ensures that with the specimen geometries studied, the crack driving force decreases with increasing crack length guaranteeing arrest (Gates 1976).

Although such a system offers many practical testing advantages it is not a good representation of the effects of thermal stresses driving a crack through a pressure vessel wall (ASME XI 1977). Here, the crack is assumed to initiate from a sharp defect and crack growth results from the increasing driving force. Arrest results from the crack running into hotter and thus tougher material. It is uncertain as to which parameters associated with crack propagation and arrest are materials constants and it is possible that the loading system may influence the data obtained. Tests have therefore been performed where machine interaction together with sharp notched specimens resulted in a crack driving force which increased with increasing crack length. Material properties were constant in each specimen so that although the tests did not simulate this variable, the tests were still closer to the practical case than the blunt notched tests.

## TEST DETAILS

Specimens were machined from a tool steel of approximate composition 1.0%C, 1.3%Mn, 0.5%Cr, 0.5%W, 0.2%V, 0.3%Si to two geometries shown in Fig. 1. Specimens of series A were nominally the same. Specimens of series B fell into two groups. One set had a similar heat treatment but different starting notch depths, $a_o$. The other had similar starting notch depth but a range of heat treatments designed to produce different toughnesses. The relevant details are given in Table I. Sharp notches were produced by fatigue pre-cracking using a maximum stress intensity factor of 15MPa $m^{½}$. Specimens were subsequently side grooved on one face to guide the crack. The opposite face was coated with a thin insulating layer of epoxy followed by a vapour deposited aluminium ladder gauge. The growing crack broke successive rungs of the ladder and the resulting loss of electrical continuity was used to monitor the crack position (Gates 1976). The first rung was only 5mm beyond the crack tip so that initial growth could be monitored accurately.

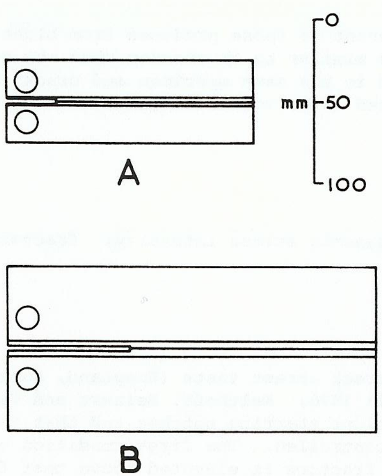


Fig. 1. Dimensions of Test Specimens

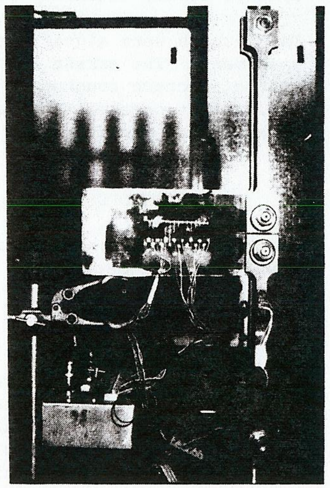

Fig. 2. Test Apparatus

Specimens were loaded in series with a set of compliant pull rods into a hard screw driven testing machine, Fig. 2. The pull rod compliance had little effect on crack growth, probably because the machine compliance dominated that of the pull rods (Gates 1976). However, they had the advantage that strain gauges could be fixed to the pull rods and calibrated against load so that dynamic load could also be



monitored during fast crack growth.

Fourth order polynomials were fitted to the time dependencies of both load and crack length data and used in a dynamic finite difference computer program (Gates 1978a) that calculated the instantaneous stress intensity factor. In this case a 1-dimensional finite difference program based on that developed at Battelle Columbus (Kanninen 1974; Genlen, Popelar and Kanninen 1979) was used.

## RESULTS

Crack growth rates indicated by the ladder gauges were non-uniform. The cracks tended to accelerate, run at a constant velocity and then decelerate. In the B series specimens the crack subsequently arrested whereas in the A series specimens a second acceleration was noted and simultaneously the crack started to run out of its original plane in a direction ar right angles to the original path. It was thus assumed that an intermediate arrest occurred in the A series specimens prior to the second acceleration and change in crack direction.

A linear least squares fit was applied to the crack growth data to determine the mean crack speeds (V Average) given in Table 1. Crack speeds were generally higher

TABLE 1 Test Details and Arrest Toughnesses

| Specimen Number | $a_o$ mm | $K_{IC}$ MPa $m^{½}$ | V Average m/s | $K_{Ia}$ (dynamic) MPa $m^{½}$ | $K_{Ia}$ (static) MPa $m^{½}$ From $K_{IS}$ | From Machine |
|---|---|---|---|---|---|---|
| A16 | 16.7 | 43.4 | 212 | 46-52 | 42.0 | |
| A20 | 13.5 | 33.0 | 134 | 56-64 | 42.0 | |
| A21 | 15.0 | 38.6 | 195 | 49-56 | 47.0 | |
| A22 | 14.5 | 36.1 | 267 | 65-75 | 39.0 | |
| A23 | 12.5 | 31.2 | 153 | 52-57 | 40.0 | |
| A24 | 13.5 | 41.8 | 294 | 71-76 | 56.0 | |
| A25 | 14.5 | 40.3 | 262 | 55-64 | 49.5 | |
| A26 | 14.0 | 33.5 | 200 | 55-65 | 31.0 | |
| B1* | 80.5 | 57.7 | 15 | 51-63 | 52.5 | |
| B2* | 96.0 | 52.5 | 58 | 50-55 | 51.0 | 49.3 |
| B3* | 64.5 | 57.4 | 142 | 46-52 | 55.6 | |
| B5 | 43.5 | 40.0 | 86 | 47-52 | 44.9 | 47.8 |
| B6 | 22.0 | 41.4 | 213 | 68-85 | 64.2 | 64.9 |
| B15 | 59.0 | 44.0 | 71 | 54-60 | 47.0 | 51.6 |
| B19 | 56.0 | 92.0 | 76 | 115-145 | 105.9 | 101.8 |
| B20* | 66.0 | 61.0 | 37 | 66-75 | 64.8 | 68.7 |
| B21 | 57.6 | 49.0 | 40.5 | 54-70 | 53.7 | 50.6 |

* These tests were less dynamic than the remaining specimens

(134-294m/s) in series A specimens than those in series B (15-213 m/s).

Dynamic stress intensity factors ($K_{ID}$) were computed from the instantaneous crack length and specimen load and examples are shown in Fig. 3a,b,c compared with static stress intensity factors ($K_{IS}$) computed from the initial load and static machine and specimen compliances (Gates 1976). The calculated values of $K_{ID}$ were subject to numerical "noise" and appear distributed at random about a mean trend. In all tests of series A (e.g. Fig.3a) and most of series B (e.g. Fig. 3b), $K_{ID}$ increased more rapidly with increasing crack length than $K_{IS}$. In some of the tests in series

B (e.g. Fig. 3c) which had a lower velocity, $K_{ID}$ initially dropped below $K_{IS}$ before rising above it. Such specimens are marked by an asterisk in Table 1.

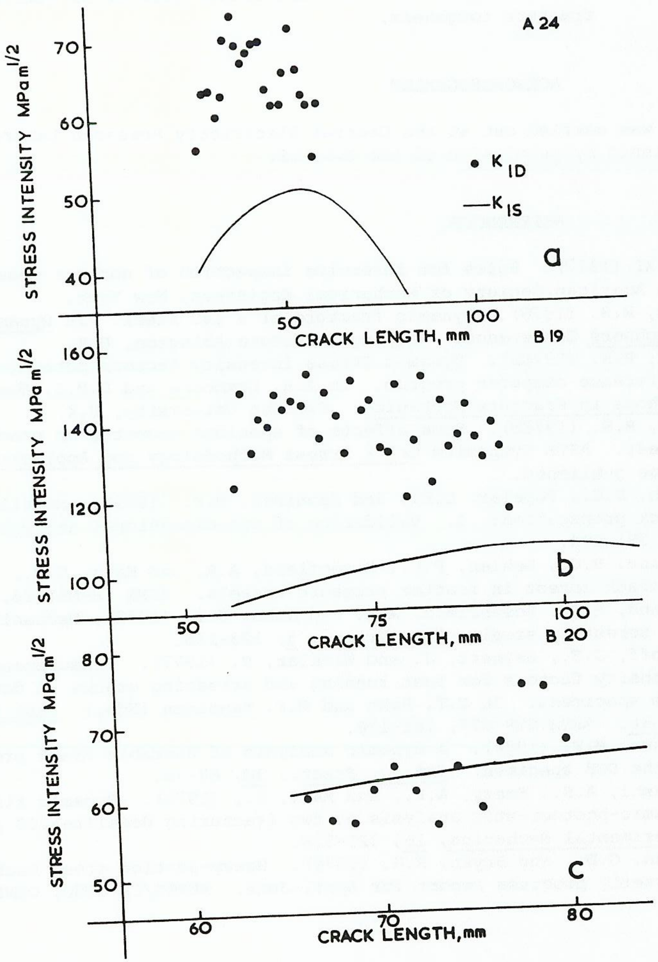


Fig. 3. A comparison of dynamic and static stress intensity factors

Values of the dynamic toughness at the instant of arrest, $K_{Ia}$(dynamic) were determined from the value of $K_{ID}$ at arrest for the series B specimens and for the assumed intermediate arrest for the series A specimens. This was indicated by zero crack velocity to within the accuracy of the numerical differentiation of the crack length/time data. Values of $K_{Ia}$(dynamic) could only be determined to within the



scatter band reflecting the numerical noise evident in the $K_{ID}$ values shown in Figure 3. Except for 1 specimen of series B the values were all greater than $K_{IC}$ determined from the same specimens, Table 1 and Fig. 4. The static crack arrest toughness, $K_{Ia}$(static) was determined from the value of $K_{IS}$ at the arrested crack length and the values are given in Table 1. These are compared with similar values, Table 1, determined from the load recorded on the test machine and the crack length at arrest with good agreement between the two values. Values of the $K_{Ia}$(static) were either similar to or greater than $K_{IC}$, Fig. 4.

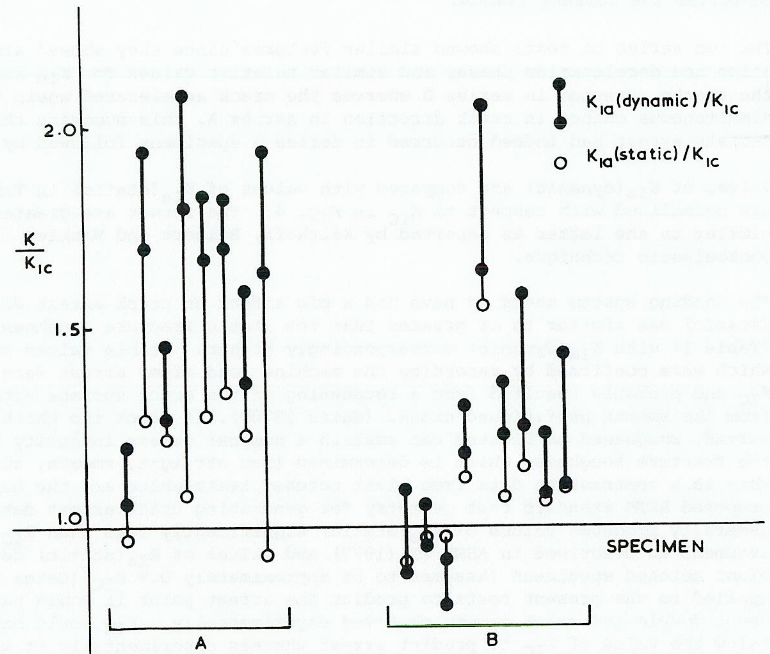


Fig. 4 A comparison of dynamic and static crack arrest toughnesses

## DISCUSSION

Unlike the results from current experiments, cracks initiated from blunt starting notches tended to reach their highest velocity shortly after initiation with only a slight deceleration afterwards (Hoagland, Rosenfield and Hahn 1972; Gates 1978b). This was a different characteristic to the present tests where the initial acceleration was more gradual. Crack velocities, Table 1, were all much lower than those found for similar material but with blunt notched specimens tested in a hard test rig (Gates 1978b) where crack speeds between 439 and 629 m/s were reported. Since the present tests are a better representation of the effects of thermal stresses it suggests that if the initial defects are sharp, crack speeds may also be low in pressure vessels and the results closer to the predictions of a static analysis. The values of $K_{ID}$ from the specimens with the lowest crack speeds (e.g.

Fig. 3c) were indeed closer to $K_{IS}$.

The computed values of $K_{ID}$ were subject to the numerical "noise" shown in Figure 3. This noise was not evident in previous computations with the same program on data from blunt notched tests and probably resulted from the extra input data on specimen load required here. Previous analyses with the same computer program and similar specimen material (Gates 1978b) but using blunt notched specimens indicated that $K_{Ia}$(dynamic) > $K_{Ia}$(static) < $K_{IC}$. This was similar to the results of Kalthoff and others (1977) for blunt notched tests. Thus the computer program indicates the correct trends.

The two series of tests showed similar features since they showed similar acceleration and deceleration phases and similar relative values for $K_{ID}$ and $K_{IS}$. Since the cracks arrested in series B whereas the crack accelerated again with a simultaneous change in crack direction in series A, this suggests that an intermediate arrest had indeed occurred in series A specimens followed by reinitiation.

Values of $K_{Ia}$(dynamic) are compared with values of $K_{Ia}$(static) in Table 1 and both are normalised with respect to $K_{IC}$ in Fig. 4. The former are greater than or similar to the latter as reported by Kalthoff, Beinert and Winkler (1977) using a photoelastic technique.

The loading system seems to have had a big effect on crack arrest data since $K_{Ia}$ (static) was similar to or greater than the static fracture toughness, $K_{IC}$, (Table 1) with $K_{Ia}$(dynamic) correspondingly higher. Stable values of $K_{Ia}$(static) which were confirmed by recording the machine load after arrest were greater than $K_{IC}$ and probably resulted from a roughening of the crack surface after initiation from the smooth prefatigued crack. (Gates 1978b). A crack tip which is either curved, roughened or blunted can sustain a nominal stress intensity factor above the fracture toughness which is determined from straight, smooth, sharp cracks. This is a contrast to data from blunt notched tests which are the basis for the proposed ASTM standard test geometry for generating crack arrest data. This generally produced values of $K_{Ia}$(static) significantly less than $K_{IC}$. Had a static argument as described in ASME XI (1977) and values of $K_{Ia}$(static) determined from blunt notched specimens (assumed to be approximately 0.9 $K_{IC}$ (Gates 1978b)) been applied to the present tests to predict the arrest point it would have predicted about double the crack growth observed experimentally. $K_{IS}$ would have had to fall below the value of $K_{IC}$ to predict arrest whereas experimentally it was close to the peak in $K_{IS}$. Crack growth is the most sensitive parameter to indicate the magnitude of $K_{Ia}$(static) and the amount of crack growth observed in the present tests confirms that $K_{Ia}$(static) was greater than $K_{IC}$.

The present tests suggest that if the arrest point can be determined from a static analysis, then since the present tests partially simulate thermal stresses in a pressure vessel, laboratory data determined from blunt notched specimens may be conservative when applied to pressure vessels. It has been suggested (Hoagland and others 1978) that a dynamic analysis is necessary so that kinetic energy effects that help to maintain crack growth are taken account of. The present data may help to counteract this effect. Limited confirmation of these effects are indicated in the TSE-5 simulated LOCA test performed at Oak Ridge Laboratories (Whitman and Bryan 1979). In this test the crack initiated and arrested in three stages and in the first two $K_{IS}$ was rising. The values of $K_{Ia}$(static) deduced from finite element analyses were close to $K_{IC}$ for the arrest temperature.

## CONCLUSIONS

Crack arrest tests with specimens with sharp initial defects and a loading system that produced a crack driving force that initially increased with increasing crack length produced the following results.



(a) Crack velocities low in comparison with those produced in blunt notched specimens

(b) Dynamic arrest toughnesses at the instant of arrest greater than the static stress intensity factors recorded after arrest.

(c) Arrest toughnesses that were either greater or similar to the static fracture toughness.

## ACKNOWLEDGEMENT

This was carried out at the Central Electricity Research Laboratories and is published by permission of the C.E.G.B.

## REFERENCES

ASME XI (1977). Rules for inservice inspection of nuclear power plant components. The American Society of Mechanical Engineers, New York.

Gates, R.S. (1976). Dynamic fracture of a 1%C steel. In Dynamic Fracture Toughness Conference. Welding Institute Abington, U.K.

Gates, R.S. (1978a). Dynamic Stress intensity factors determined from a finite difference computer program. In A.R. Luxmoore and D.R.J. Owen (Eds.), Numerical Methods in Fracture Mechanics. Swansea University, U.K.

Gates, R.S. (1978b). Some effects of specimen geometry on crack propagation and arrest. ASTM Symposium Crack Arrest Methodology and Applications, Philadelphia to be published.

Gehlen, P.C., Popelar, C.H., and Kanninen, M.F. (1979). Modelling of dynamic crack propagation: I. Validation of one-dimensional analysis, Int. J. Fract., 15, 281-294.

Hoagland, R.G., Gehlen, P.C., Rosenfield, A.R. and Hahn, G.T., (1978). Analysis of crack arrest in reactor pressure vessels. ASME 78-MAT-16, New York.

Hoagland, R.G., Rosenfield, A.R. and Hahn, G.T. (1972), Mechanisms of fast fracture and arrest in steels, Met. Trans., 3, 123-136.

Kalthoff, J.F., Beinert, J. and Winkler, S. (1977). Measurements of dynamic stress intensity factors for fast running and arresting cracks in double cantilever beam specimens. In G.T. Hahn and M.F. Kanninen (Eds.) Fast Fracture and Crack Arrest. ASTM STP 627, 161-176.

Kanninen, M.F. (1974). A dynamic analysis of unstable crack propagation and arrest in the DCB specimen. Int. J. Fract., 10, 67-78.

Kobayashi, A.S., Emery, A.F., and Mall, S., (1976). Dynamic finite-element and dynamic-photoelastic analysis of two fracturing Homalite-100 plates. Experimental Mechanics, 16, 321-328.

Whitman, G.D., and Bryan, R.H. (1979). Heavy-section steel technology, Program quarterly progress report for April-June. NUREG/CR-0980, ORNL/NUREG/TN-347.

Fig. 3c) were indeed closer to $K_{IS}$.

The computed values of $K_{ID}$ were subject to the numerical "noise" shown in Figure 3. This noise was not evident in previous computations with the same program on data from blunt notched tests and probably resulted from the extra input data on specimen load required here. Previous analyses with the same computer program and similar specimen material (Gates 1978b) but using blunt notched specimens indicated that $K_{Ia}$(dynamic) > $K_{Ia}$(static) < $K_{IC}$. This was similar to the results of Kalthoff and others (1977) for blunt notched tests. Thus the computer program indicates the correct trends.

The two series of tests showed similar features since they showed similar acceleration and deceleration phases and similar relative values for $K_{ID}$ and $K_{IS}$. Since the cracks arrested in series B whereas the crack accelerated again with a simultaneous change in crack direction in series A, this suggests that an intermediate arrest had indeed occurred in series A specimens followed by reinitiation.

Values of $K_{Ia}$(dynamic) are compared with values of $K_{Ia}$(static) in Table 1 and both are normalised with respect to $K_{IC}$ in Fig. 4. The former are greater than or similar to the latter as reported by Kalthoff, Beinert and Winkler (1977) using a photoelastic technique.

The loading system seems to have had a big effect on crack arrest data since $K_{Ia}$ (static) was similar to or greater than the static fracture toughness, $K_{IC}$, (Table 1) with $K_{Ia}$(dynamic) correspondingly higher. Stable values of $K_{Ia}$(static) which were confirmed by recording the machine load after arrest were greater than $K_{IC}$ and probably resulted from a roughening of the crack surface after initiation from the smooth prefatigued crack. (Gates 1978b). A crack tip which is either curved, roughened or blunted can sustain a nominal stress intensity factor above the fracture toughness which is determined from straight, smooth, sharp cracks. This is a contrast to data from blunt notched tests which are the basis for the proposed ASTM standard test geometry for generating crack arrest data. This generally produced values of $K_{Ia}$(static) significantly less than $K_{IC}$. Had a static argument as described in ASME XI (1977) and values of $K_{Ia}$(static) determined from blunt notched specimens (assumed to be approximately 0.9 $K_{IC}$ (Gates 1978b)) been applied to the present tests to predict the arrest point it would have predicted about double the crack growth observed experimentally. $K_{IS}$ would have had to fall below the value of $K_{IC}$ to predict arrest whereas experimentally it was close to the peak in $K_{IS}$. Crack growth is the most sensitive parameter to indicate the magnitude of $K_{Ia}$(static) and the amount of crack growth observed in the present tests confirms that $K_{Ia}$(static) was greater than $K_{IC}$.

The present tests suggest that if the arrest point can be determined from a static analysis, then since the present tests partially simulate thermal stresses in a pressure vessel, laboratory data determined from blunt notched specimens may be conservative when applied to pressure vessels. It has been suggested (Hoagland and others 1978) that a dynamic analysis is necessary so that kinetic energy effects that help to maintain crack growth are taken account of. The present data may help to counteract this effect. Limited confirmation of these effects are indicated in the TSE-5 simulated LOCA test performed at Oak Ridge Laboratories (Whitman and Bryan 1979). In this test the crack initiated and arrested in three stages and in the first two $K_{IS}$ was rising. The values of $K_{Ia}$(static) deduced from finite element analyses were close to $K_{IC}$ for the arrest temperature.

## CONCLUSIONS

Crack arrest tests with specimens with sharp initial defects and a loading system that produced a crack driving force that initially increased with increasing crack length produced the following results.



(a) Crack velocities low in comparison with those produced in blunt notched specimens

(b) Dynamic arrest toughnesses at the instant of arrest greater than the static stress intensity factors recorded after arrest.

(c) Arrest toughnesses that were either greater or similar to the static fracture toughness.

## ACKNOWLEDGEMENT

This was carried out at the Central Electricity Research Laboratories and is published by permission of the C.E.G.B.

## REFERENCES

ASME XI (1977). Rules for inservice inspection of nuclear power plant components. The American Society of Mechanical Engineers, New York.

Gates, R.S. (1976). Dynamic fracture of a 1%C steel. In Dynamic Fracture Toughness Conference. Welding Institute Abington, U.K.

Gates, R.S. (1978a). Dynamic Stress intensity factors determined from a finite difference computer program. In A.R. Luxmoore and D.R.J. Owen (Eds.), Numerical Methods in Fracture Mechanics. Swansea University, U.K.

Gates, R.S. (1978b). Some effects of specimen geometry on crack propagation and arrest. ASTM Symposium Crack Arrest Methodology and Applications, Philadelphia to be published.

Gehlen, P.C., Popelar, C.H., and Kanninen, M.F. (1979). Modelling of dynamic crack propagation: I. Validation of one-dimensional analysis, Int. J. Fract., 15, 281-294.

Hoagland, R.G., Gehlen, P.C., Rosenfield, A.R. and Hahn, G.T., (1978). Analysis of crack arrest in reactor pressure vessels. ASME 78-MAT-16, New York.

Hoagland, R.G., Rosenfield, A.R. and Hahn, G.T. (1972), Mechanisms of fast fracture and arrest in steels, Met. Trans., 3, 123-136.

Kalthoff, J.F., Beinert, J. and Winkler, S. (1977). Measurements of dynamic stress intensity factors for fast running and arresting cracks in double cantilever beam specimens. In G.T. Hahn and M.F. Kanninen (Eds.) Fast Fracture and Crack Arrest. ASTM STP 627, 161-176.

Kanninen, M.F. (1974). A dynamic analysis of unstable crack propagation and arrest in the DCB specimen. Int. J. Fract., 10, 67-78.

Kobayashi, A.S., Emery, A.F., and Mall, S., (1976). Dynamic finite-element and dynamic-photoelastic analysis of two fracturing Homalite-100 plates. Experimental Mechanics, 16, 321-328.

Whitman, G.D., and Bryan, R.H. (1979). Heavy-section steel technology, Program quarterly progress report for April-June. NUREG/CR-0980, ORNL/NUREG/TN-347.